Quaternary Science Reviews 161 (2017) 18–29

Contents lists available at ScienceDirect

Quaternary Science Reviews

journal homepage: www.elsevier.com/locate/quascirev

Multi-proxy evidence of millennial climate variability from multiple Bahamian speleothems

Monica M. Arienzo [a, b, *], Peter K. Swart [a], Kenneth Broad [c], Amy C. Clement [d], Ali Pourmand [a], Brian Kakuk [e]

[a] Department of Marine Geosciences, Rosenstiel School of Marine and Atmospheric Science, University of Miami, 4600 Rickenbacker Causeway, Miami, FL, USA
[b] Now at Division of Hydrologic Sciences, Desert Research Institute, Reno, NV, USA
[c] Department of Marine Ecosystems and Society, Rosenstiel School of Marine and Atmospheric Science, University of Miami, 4600 Rickenbacker Causeway, Miami, FL, USA
[d] Department of Atmospheric Sciences, Rosenstiel School of Marine and Atmospheric Science, University of Miami, 4600 Rickenbacker Causeway, Miami, FL, USA
[e] Bahamas Underground, Marsh Harbor, Bahamas

ARTICLE INFO

Article history:
Received 5 October 2016
Received in revised form
30 January 2017
Accepted 2 February 2017

ABSTRACT

Northern Hemisphere tropical paleoclimate records support significant changes associated with Dansgaard Oeschger (D/O) events and Heinrich stadials 1 to 6 during the last 64,000 years. However, few absolutely dated terrestrial records from the western Atlantic span the last six Heinrich stadials. Here we present geochemical results from three new stalagmites collected from a cave in the Bahamas which encompass Heinrich stadials 1 to 6. We build on a previous study of the $\delta^{13}C$ and $\delta^{18}O$ values of the calcite and $\delta^{18}O$ value of fluid inclusions from a single stalagmite from the same cave spanning the last three Heinrich stadials. Absolute geochronometry using U-Th equilibrium series demonstrates that the stalagmites formed between 63.8 and 13.8 kyr BP. The $\delta^{13}C$ and $\delta^{18}O$ values of the calcite show higher values associated with Heinrich stadials 1–6, and lower values during the D/O interstadial events. The Sr/Ca ratios of the calcite are shown to be relatively invariant, while in two of the samples the Mg/Ca ratios track the $\delta^{13}C$ values.

Increases in the $\delta^{18}O$ values across Heinrich stadials 1–6 are interpreted as being driven by lower temperatures. The two deeper occurring stalagmites demonstrate increased Mg/Ca ratios and $\delta^{13}C$ values during Heinrich stadials 1 and 2 which are interpreted as a signal of reduced flow rates in the epikarst and increased water/rock interactions as a result of increased aridity which potentially occurred across all six Heinrich stadials. The observed reductions in mean annual temperature and amount of precipitation across Heinrich stadials are proposed to be driven by a reduction in sea surface temperatures in the North Atlantic and an expanded Bermuda High. During D/O interstadials, the Bahamas cave records likely indicate warmer and/or wetter climate; however the isotopic shifts are not as significant as the isotopic excursions associated with Heinrich stadials.

1. Introduction

Millennial scale, rapid climate change events such as Dansgaard/Oeschger (D/O) and Heinrich stadial events have been significant drivers of climate variability over the last 64,000 years (Bond et al., 1997; Dansgaard et al., 1984). Studies from the Northern Hemisphere tropical western Atlantic have documented rapid hydrologic and temperature changes associated with D/O and Heinrich stadials (Escobar et al., 2012; Grimm et al., 2006; Hagen and Keigwin, 2002; Hodell et al., 2012; Keigwin and Jones, 1994; Lozano-Garcia et al., 2015; Sachs and Lehman, 1999), however few high resolution records span the last 64,000 years from this region (Deplazes et al., 2013; Grimm et al., 2006; Peterson et al., 2000). This study spans the last 64,000 years, demonstrating climatic changes associated with D/O events and the last six Heinrich stadials, and adds to the

* Corresponding author. Division of Hydrologic Sciences, Desert Research Institute, 2215 Raggio Parkway, Reno, NV, USA.
E-mail address: marienzo@dri.edu (M.M. Arienzo).

http://dx.doi.org/10.1016/j.quascirev.2017.02.004
0277-3791/

scarce absolutely dated terrestrial records from the western Atlantic.

The goal of this study was to build upon a previous Bahamian stalagmite record (Arienzo et al., 2015) by analyzing three additional stalagmites spanning the last 64,000 years in order to reconstruct millennial scale climate variations using multiple geochemical proxies. The study of Arienzo et al. (2015) utilized the $\delta^{18}O$ values of the fluid inclusions ($\delta^{18}O_w$) and showed that the main driver of increased $\delta^{18}O$ values of the calcite ($\delta^{18}O_c$) associated with Heinrich stadials 1 to 3 was temperature rather than changes in the $\delta^{18}O$ value of the fluid. Increased $\delta^{13}C$ values of the carbonate ($\delta^{13}C_c$) were also observed associated with Heinrich stadials, driven by either a decrease in temperature or an increase in aridity. Both a decrease in temperature and an increase in aridity can lead to a reduced biogenic CO_2 component of the dissolved inorganic calcite (DIC) and more positive $\delta^{13}C_c$ values (Genty et al., 2003; Arienzo et al., 2015). Here, we examine the role of Northern Hemisphere climate on the tropics by combining multiple geochemical proxies including stable isotopes of the calcite and minor element measurements from four stalagmites from one cave to determine the robust signals of climatic drivers in this region during the last 64,000 years. We then compare the results from the Bahamas to ocean sediment, ice core and tropical speleothem records, to place the Bahamas records in a regional setting, to better characterize the western Atlantic climatic response associated with such rapid climate events, and to understand the global propagation of rapid climate events.

1.1. Millennial scale climate

The D/O and Heinrich stadial events were rapid climate events with a global climate response (Deplazes et al., 2013; Grimm et al., 2006; Peterson et al., 2000). Heinrich stadials were associated with cooling in the North Atlantic, the southerly expansion of ice, freshwater discharge to the North Atlantic, and reduced North Atlantic deep water formation and a slow/shut down of the Atlantic meridional overturning circulation (AMOC) (Broecker et al., 1985; Henry et al., 2016; McManus et al., 2004), with a global climate response (Clement and Peterson, 2008).

The D/O interstadials were recorded in the Greenland ice cores as periods of warming, followed by a gradual return to cooler temperatures (Dansgaard et al., 1984). The D/O stadials have been shown to be associated with a reduction in AMOC (Henry et al., 2016). While D/O events were global in their scale (Fletcher et al., 2010; Jiménez-Moreno et al., 2010; Jouzel et al., 2007; Siddall et al., 2010), the mechanisms which drove these events and their global propagation are still not well understood (Clement and Peterson, 2008; Timmermann et al., 2003). Several hypotheses have been proposed including changes in the AMOC (Broecker et al., 1985), sea ice coverage (Li et al., 2010; Petersen et al., 2013), tropical processes (Clement and Cane, 1999), and the Southern Ocean (Buizert and Schmittner, 2015).

2. Regional setting and sample specimens for study

The modern climate of the subtropical Bahamas is primarily controlled by the easterly trade winds with minimal annual air temperature variation of 22–28 °C (Baldini et al., 2007). There are distinct wet and dry seasons with the wetter period between late spring to early winter driven by the Bermuda High (Baldini et al., 2007).

For this study, four stalagmites (AB-DC-01, 03, 09, and 12) were collected from a currently submerged cave located in the middle of southern Abaco Island, Bahamas (N26°14, W77°10) (Fig. 1 a & b). These speleothems formed during previous sea level low-stands in caves of Pleistocene limestone aeolianites and marine limestones (Arienzo et al., 2015; Walker et al., 2008). In addition, dolomite has been reported in the subsurface of Abaco Island at a depth of ~24 m below the surface (Kaldi and Gidman, 1982). The cave was accessed through a collapsed sinkhole and consists of laterally extensive levels at ~22, 33.5 and 45 m below sea level. These stalagmites (AB-DC-01, 03, 09, and 12) were obtained from water depths respectively of 33.5, 34.4, 16.5, and 11.9 m below current sea level. Results from AB-DC-09 have been presented previously (Arienzo et al., 2015).

3. Stalagmite geochemistry

The isotopic composition of oxygen and carbon from the carbonate of stalagmites are routinely measured as proxies for paleoclimate reconstructions. However, the interpretation of these isotopes is inherently complex as a result of the influence of temperature and water composition. Specifically, the $\delta^{18}O$ values of the carbonate are thought to reflect either the $\delta^{18}O$ value of the rainfall or the temperature of the cave (Arienzo et al., 2015; Kanner et al., 2012). Alternatively, many studies have relied on additional proxies, such as isotopic analyses of fluid inclusions, trace and minor elemental analysis and modern cave monitoring (Fairchild and Baker, 2012).

The $\delta^{13}C$ values of the carbonate can be impacted by biological soil activity, the type and quantity of vegetation (C_3 versus C_4), Prior Calcite Precipitation (PCP), and the amount of water/rock interaction (Fairchild et al., 2006). These factors can be further influenced by changes in temperature and the amount of precipitation. Within caves with active speleothem formation, it has been demonstrated that ventilation may influence the $\delta^{13}C$ value of the CO_2, and hence the $\delta^{13}C_c$ value of the speleothem calcite (Lambert and Aharon, 2011; Tremaine et al., 2011). In addition, changes in the $\delta^{13}C_c$ and $\delta^{18}O_c$ values of speleothems may not be solely driven by climatic factors, but rather by kinetic factors. Two tests have been suggested to account for such effects. The 'Hendy' test (Hendy, 1971) examines whether there is lateral variability along growth bands in the isotope record which if present suggests non-equilibrium precipitation, while an alternate approach is to conduct replication tests (Mühlinghaus et al., 2009), in which multiple stalagmites from the same cave are measured to replicate geochemical trends that can be associated with climatic factors (Dorale and Liu, 2009).

The trace and minor elemental (Mg, Sr, Fe, Ba) concentrations of speleothems have increasingly proven to be important in the understanding of environmental processes affecting speleothem growth (Cross et al., 2015; Cruz et al., 2007; Tremaine and Froelich, 2013). Factors that can influence the incorporation of minor elements into drip water include the type of overlying bedrock (Fairchild et al., 2000), hydrologic conditions (Cruz et al., 2007), routing path of the water (Fairchild and Treble, 2009), amount of water/rock interaction (Fairchild et al., 2000), cave ventilation (Wong et al., 2011), and calcite precipitation rate (Lorens, 1981). During periods of enhanced aridity, PCP can occur through evaporation or CO_2 degassing in the epikarst or within the cave ceiling (Treble et al., 2015). With increasing PCP, drip waters become enriched in Mg and Sr as these elements are excluded from the solid phase. Evidence of PCP, and hence increased aridity, have been attributed to a positively correlated Mg to Sr variation in speleothems (Fairchild and Treble, 2009). In addition, during periods of low flow, increased residence time of waters in the epikarst leads to increased water/rock interaction and hence elevated minor

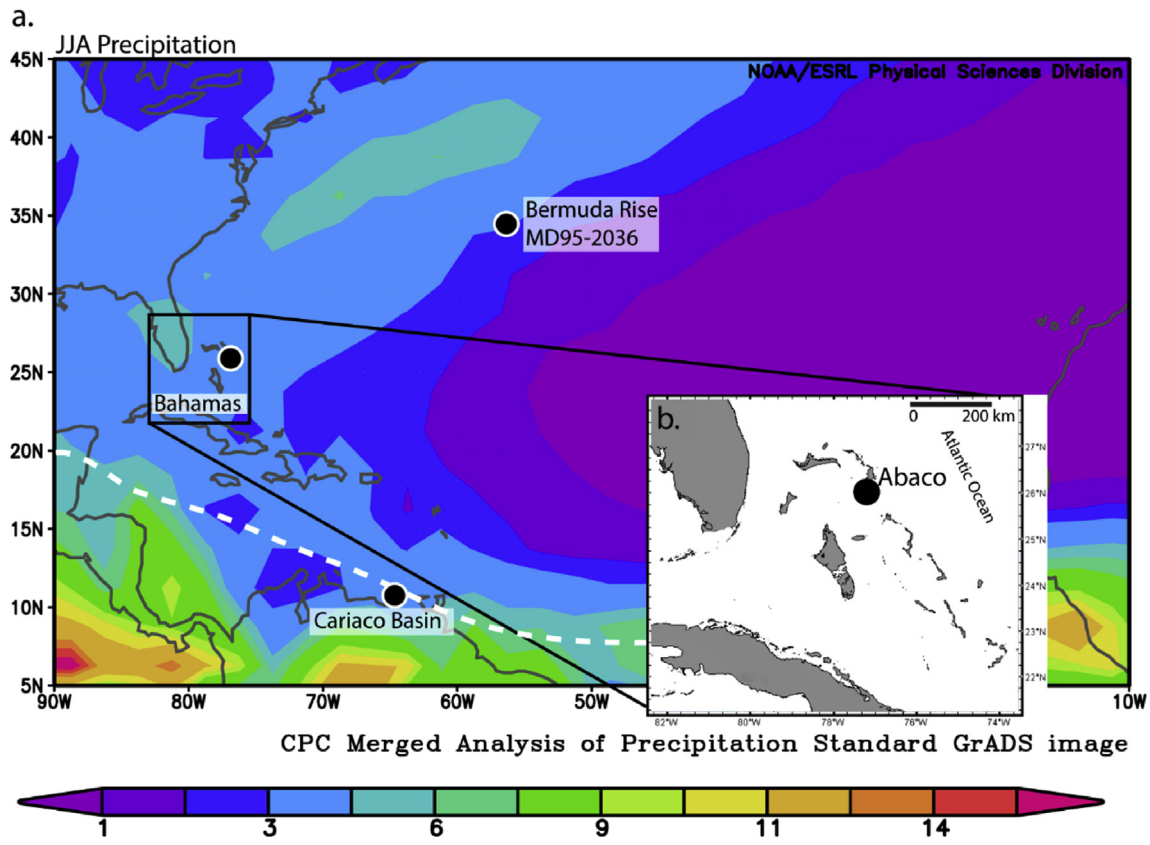

Fig. 1. Map of the Atlantic (a) showing the locations of the Bahamas, Cariaco Basin (Deplazes et al., 2013) and Bermuda Rise (Core MD95-2036) (Sachs and Lehman, 1999). Contours show the modern June-July-August (JJA) mean precipitation rate (mm/day) from the Climate Prediction Center Merged Analysis of Precipitation (CMAP) from 1979 to 2016 CE. The white dotted line is the approximate location of the Intertropical Convergence Zone (ITCZ) during the boreal summer. b) Close up of the Bahamas. The submerged stalagmites were collected from Abaco Island, Bahamas from depths ranging from 11.9 to 34.4 m below sea level.

element concentrations (Fairchild and Treble, 2009).

4. Methods

To prepare the stalagmites for geochemical subsampling, the samples were encased in epoxy, cut along the center growth axis, and polished (Supplementary Fig. 1). All stalagmites exhibited dense calcite with no evidence of diagenetic alteration along the central axis where the subsamples analyzed for the geochemical parameters were taken.

4.1. Absolute geochronometry using Uranium-Thorium decay series

A total of 27 samples were processed for U-Th geochronometry. Approximately 0.1–0.2 g of each sample collected from the central axis of growth by hand-drilling were dissolved in 6 mol/l nitric acid, spiked with IRMM-3636a, and processed through extraction chromatography to separate U and Th. The isotope ratios were measured on a Thermo Fisher-Neptune Plus multi-collector ICP-MS at the University of Miami. The details of U-Th geochronometry and the propagation of random and systematic uncertainties are provided in Pourmand et al. (2014). In the previous and current studies, uncertainties for the ages are reported at 95% confidence interval (CI) based on Monte Carlo simulations. For all U-Th samples, an initial $^{230}Th/^{232}Th$ activity ratio of 3.7 ± 0.6 was used to account for excess (unsupported) ^{230}Th (Arienzo et al., 2015). Arienzo et al. (2015) determined this value by comparing initial $^{230}Th/^{232}Th$ measurements from modern Bahamian cave calcites to previously published values from the Bahamas (Hoffmann et al., 2010; Beck et al., 2001) with an initial $^{230}Th/^{232}Th$ activity ratio of 3.7 ± 0.6 falling within the range of values observed for the Bahamas. All ages are reported in years before present (yr BP), 2013 CE.

4.2. Carbon and oxygen isotopes

Sampling of the speleothem carbonate for carbon and oxygen isotopes was carried out using a New-Wave computerized micro-mill at both high and low resolution. Low resolution sampling consisted of one sample every 1000 μm throughout the length of the stalagmite. Two areas were analyzed at high resolution (20 μm sampling interval) for stalagmite AB-DC-12 as these areas were thought to consist of rapid and significant isotopic shifts (Supplementary Fig. 1). The C and O isotopic measurements were made using a Kiel III interfaced with a Thermo-Finnigan Delta Plus Mass Spectrometer at the University of Miami. All data have been corrected for interferences at mass 45 and 46 and are reported relative to Vienna Pee Dee Belemnite (VPDB). The precision of the $\delta^{13}C_c$ and $\delta^{18}O_c$ values was better than 0.1‰.

4.3. Minor elements

Splits of material sampled from AB-DC-01, 03, and 12 analyzed for $\delta^{13}C_c$ and $\delta^{18}O_c$ were additionally measured for minor elements (Sr, Mg and Ca) utilizing a Varian Vista-Pro Inductively Coupled Plasma Optical Emission Spectrometer (ICP-OES) at the University of Miami. For stalagmite AB-DC-09, elemental sampling was conducted separately at a resolution of one sample every 500 μm. Samples were diluted in 4% trace grade HNO_3 to yield a

Table 1
U-Th dating results from a) AB-DC-01, b) AB-DC-03, and c) AB-DC-12. Ratios in brackets are activities.

Distance from Top μm	^{238}U (ppb)	(95% CI) ±	^{232}Th (ppb)	(95% CI) ±	[^{230}Th/^{238}U] (activity)	(95% CI) ±	[^{230}Th/^{232}Th] (activity)	(95% CI) ±	Uncorr. Age (yr)	(95% CI) ±	[^{234}U/^{238}U] initial (corrected activity)	(95% CI) ±	Corr. Age (yr)	(95% CI) ±
a.														
5000	112.994	0.087	2.190	0.180	0.2069	0.0037	32.7	2.74	27,397	555	0.93	0.00259	24,604	755
8000	182.614	0.104	0.531	0.016	0.2128	0.0011	223.7	6.84	26,024	138	1.004	0.00254	25,640	148
17,000	316.354	0.174	0.402	0.039	0.23	0.0012	555.3	54.07	27,798	144	1.025	0.00265	27,634	145
36,000	335.15	0.17	0.597	0.005	0.2339	0.0011	401.4	3.86	28,311	130	1.025	0.00261	28,081	136
45,000	347.287	0.212	0.316	0.006	0.2363	0.0011	792.7	16.24	28,431	127	1.032	0.00268	28,315	129
b.														
8000	566.682	0.265	2.312	0.019	0.1305	0.0006	97.7	0.9	14,925	60	1.022	0.00244	14,396	103
48,000	355.148	0.204	3.257	0.023	0.1377	0.0006	45.9	0.38	15,745	65	1.026	0.00254	14,556	202
138,000	349.702	0.161	1.345	0.021	0.1319	0.0006	104.9	1.69	15,266	57	1.012	0.00245	14,762	98
150,000	358.728	0.19	0.437	0.004	0.1347	0.0005	337.9	3.54	15,478	51	1.02	0.00248	15,320	56
178,000	389.329	0.183	0.874	0.018	0.1373	0.0006	187	3.98	15,804	65	1.019	0.00244	15,513	80
c.														
14,000	775.204	0.422	2.575	0.016	0.2914	0.0011	268.1	1.92	37,148	144	1.011	0.00264	36,712	159
53,000	260.535	0.163	0.490	0.002	0.3022	0.0014	490.8	2.88	39,247	190	1.001	0.0027	38,999	191
84,000	361.556	0.174	1.420	0.019	0.3204	0.0012	249.3	3.48	42,059	164	1.003	0.00263	41,539	180
101,000	395.053	0.351	0.311	0.002	0.3261	0.0014	1266.5	9.18	42,500	192	1.012	0.0029	42,397	191
133,000	624.8	0.29	0.271	0.007	0.3309	0.0013	2330.9	58.92	43,035	164	1.017	0.00267	42,979	164
167,000	301.034	0.192	0.390	0.004	0.336	0.0015	792	8.53	44,287	219	1.008	0.00281	44,117	219
193,000	612.42	0.275	0.240	0.006	0.3395	0.0013	2654.1	72.22	44,444	174	1.017	0.00263	44,394	174
215,000	330.759	0.2	0.553	0.031	0.3532	0.0014	646.8	36.18	47,031	206	1.01	0.00282	46,812	209
225,000	537.129	0.295	1.247	0.014	0.3648	0.0014	480.3	5.73	48,713	205	1.015	0.00279	48,410	211
228,000	319.361	0.159	0.398	0.008	0.3762	0.0015	921.8	18.78	50,999	213	1.009	0.00276	50,836	215
230,000	300.241	0.191	0.838	0.033	0.384	0.0017	420.8	16.65	52,327	269	1.009	0.00287	51,960	274
235,000	224.135	0.122	0.250	0.023	0.4072	0.0017	1118.4	101.68	56,846	276	1.004	0.00298	56,699	277
240,000	375.277	0.219	0.937	0.003	0.4202	0.0022	514.2	3.2	57,771	368	1.025	0.00285	57,449	371
256,000	209.07	0.104	0.691	0.019	0.4249	0.0017	393.2	10.86	60,592	295	0.997	0.00292	60,153	302
272,000	262.334	0.164	0.286	0.014	0.4445	0.002	1247.8	61.52	62,474	334	1.022	0.00293	62,333	335
288,000	338.949	0.155	0.361	0.006	0.4485	0.0018	1286.4	23.23	63,164	299	1.023	0.00288	63,026	300
309,000	535.342	0.255	0.672	0.010	0.4554	0.0018	1108.7	17.08	63,540	277	1.036	0.00276	63,379	276

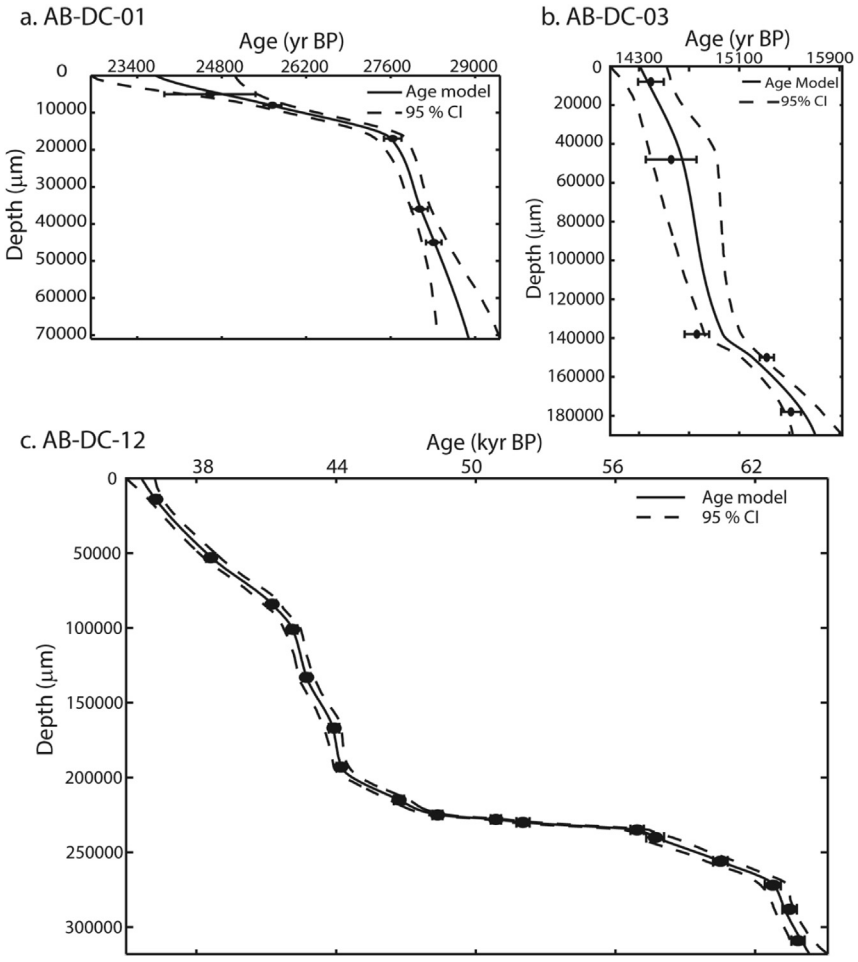

Fig. 2. Age model for samples utilized in this study, stalagmite a) AB-DC-01, b) AB-DC-03, and c) AB-DC-12. The age model for each stalagmite was calculated using the COPRA program from Breitenbach et al. (2012).

concentration of approximately 4 ppm Ca and were analyzed with standards of similar concentration and matrix.

5. Results

5.1. U-Th geochronometry

The U-Th age date results for stalagmites AB-DC-01, 03, and 12 are presented in Table 1a–c and Fig. 2. Previously, 20 U-Th age dates were acquired for stalagmite AB-DC-09 (Arienzo et al., 2015) and the results are included in Supplementary Table 1. The average error of the age determinations was ±250 years. The age model for each speleothem was calculated using the Constructing Proxy-Records from Age models (COPRA) program from Breitenbach et al. (2012) (Fig. 2). The age model was calculated in MATLAB® using the Piecewise Cubic Hermite Interpolating Polynomial (PCHIP) and 2000 Monte Carlo simulations to assign a precise timescale (Breitenbach et al. 2012).

The stalagmites formed between 63.8 and 13.8 kyr BP with a gap in the record between 36.1 and 32 kyr BP. Stalagmite AB-DC-12 was the oldest stalagmite analyzed and formed between 63.8 and 36.1 kyr BP (Fig. 2c). We note that no additional stalagmite overlaps this period therefore was not replicated. Stalagmite AB-DC-01 formed between 28.9 and 23.7 kyr BP (Fig. 2). The U-Th age from the top of this stalagmite consisted of a larger error (24,604 ± 755 yr BP), producing an error in the age model of ~ ±1000 years from 24.6 to 23.7 kyr BP (Fig. 2a). For stalagmite AB-DC-01, the ages for this stalagmite were derived from the top 4.5 cm of the sample (Table 1). As a result of minimal isotopic variability towards the base of the stalagmite, additional age dates were not pursued for this sample and therefore results in an increased age model error towards the base of the stalagmite (Fig. 2a). Stalagmite AB-DC-03 formed between 15.7 and 14.3 kyr BP and the age model exhibited an increased error from 15 to 14.6 kyr BP of ~ ±450 years driven by the age acquired at 14,762 ± 98 years which was offset from the age model (Fig. 2b). Such an offset may be due to variations in the initial ^{230}Th value as the stalagmite was forming (Arienzo et al., 2015; Cross et al., 2015). Stalagmite AB-DC-09 overlaps with stalagmites AB-DC-01 and AB-DC-03 and formed between 32 and 13.8 kyr BP (Arienzo et al., 2015) (Fig. 3). When comparing the geochemical results between stalagmites, there may be associated offsets between stalagmites because of the errors on the age models and this is discussed further in section 5.2.

5.2. Carbon and oxygen isotopes

The measured $\delta^{18}O_c$ and $\delta^{13}C_c$ values are plotted in Fig. 3 a and b versus the age model determined from the COPRA program. The $\delta^{18}O_c$ values decreased from ~ −1 to −4‰ VPDB between 62 and 37 kyr BP followed by an increasing trend from 30 to 15 kyr BP (to −0.8‰ VPDB) (Fig. 3). Stalagmite AB-DC-12 had maximum $\delta^{13}C_c$ and $\delta^{18}O_c$ values at 62.5 ± 0.3 kyr BP with positive $\delta^{13}C_c$ and $\delta^{18}O_c$

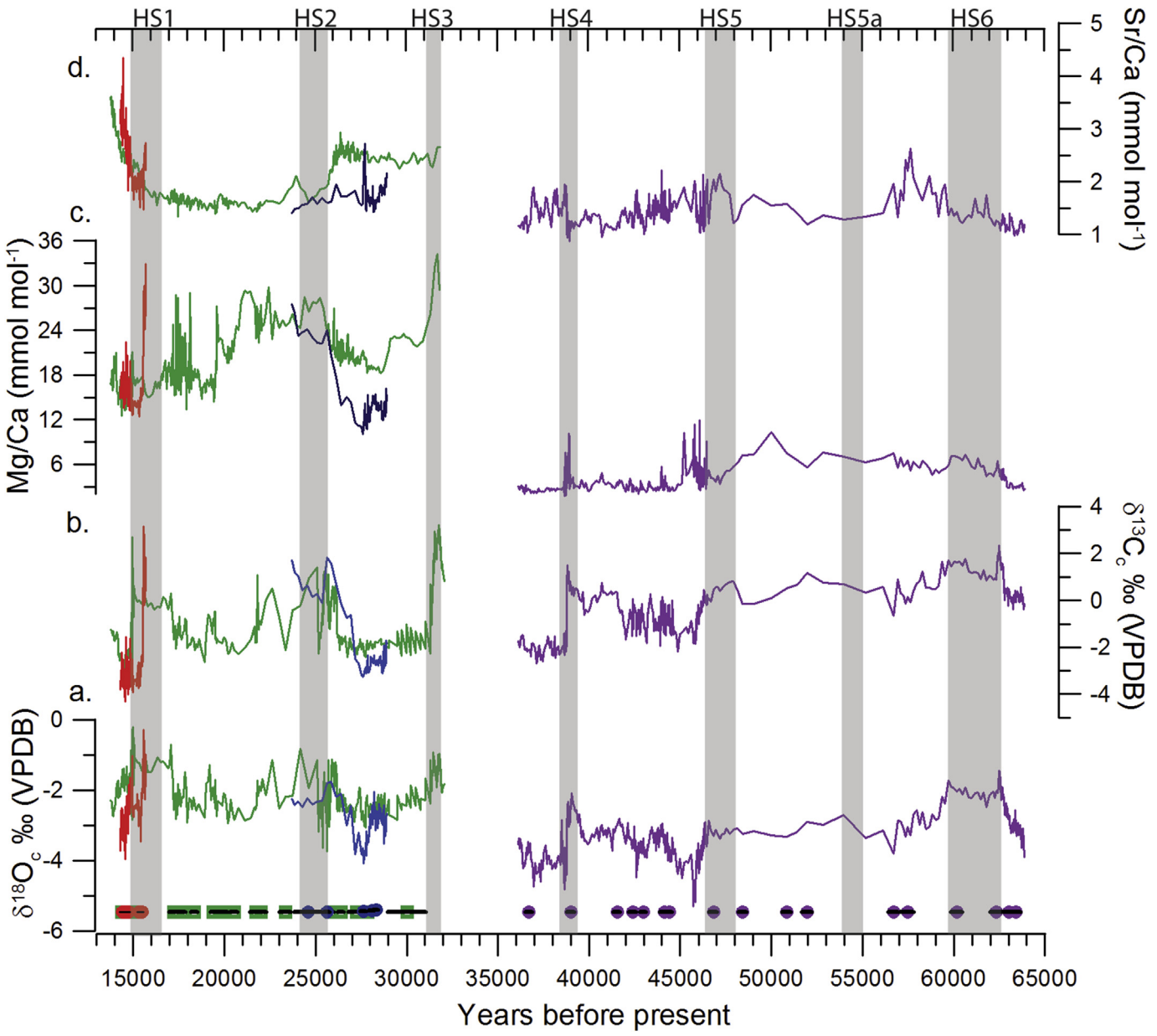

Fig. 3. Geochemical results for stalagmite AB-DC-01 (blue), AB-DC-03 (red), AB-DC-09 (dark green) and AB-DC-12 (dark purple). The $\delta^{18}O_c$ (a) and $\delta^{13}C_c$ (b) records of the carbonate demonstrate increasing values associated with Heinrich stadials 1–6. The Mg/Ca ratio (c) increases for AB-DC-01 (blue) and AB-DC-03 (red) across Heinrich stadials while the Sr/Ca ratio (d) remains relatively constant for all samples. The gray bars represent Heinrich stadials 1–6, with minimal variation in the geochemistry across Heinrich stadial 5a. (For interpretation of the references to colour in this figure legend, the reader is referred to the web version of this article.)

values at 39.7 ± 0.2 kyr BP and a minor increase at 46.5 ± 0.2 kyr BP. Increased $\delta^{13}C_c$ and $\delta^{18}O_c$ values for AB-DC-01 were observed between 26.4 and 23.6 ± 0.8 kyr BP and for AB-DC-03 $\delta^{13}C_c$ and $\delta^{18}O_c$ values increased at 15.5 ± 0.5 kyr BP. The $\delta^{13}C_c$ and $\delta^{18}O_c$ record from AB-DC-09 also showed increased values at 15 ± 0.2 and 24.5 ± 0.2 kyr BP and a minor increase in $\delta^{18}O_c$ at 31.6 ± 1 kyr BP (Arienzo et al., 2015). The timing of the increased isotopic values observed from stalagmite AB-DC-09 are offset from stalagmites AB-DC-01 and AB-DC-03. AB-DC-09 contained increased $\delta^{18}O_c$ values at 15 ± 0.2 kyr BP, ~500 years offset from the increased $\delta^{18}O_c$ values observed at 15.5 ± 0.5 kyr BP from stalagmite AB-DC-03. This difference however is within the error of the age models. Increased $\delta^{18}O_c$ values at 24.5 ± 0.2 kyr BP from AB-DC-09 are also offset from the increased $\delta^{18}O_c$ values observed between 26.4 and 23.6 ± 0.8 kyr BP from stalagmite AB-DC-01. This difference is potentially because of the increased error on the age at 24,604 ± 755 yr BP for AB-DC-01 (Fig. 2). Overall, the timing of the isotopic changes from AB-DC-01 and AB-DC-03 when compared to AB-DC-09 are within the error of the age models and the amount of change in the $\delta^{18}O_c$ values between overlapping stalagmites were similar (Fig. 3).

For speleothems AB-DC-01, -03, and −12, the Hendy test was conducted at one mm increments using a hand drill to sample laterally outwards from the central growth axis. Results demonstrated only a minimal increase from the center of the stalagmite outwards for $\delta^{13}C_c$ and $\delta^{18}O_c$ values for all the stalagmites (Supplementary Fig. 2).

5.3. Minor elements

The Mg/Ca and Sr/Ca ratios are plotted versus age (Fig. 3 c and

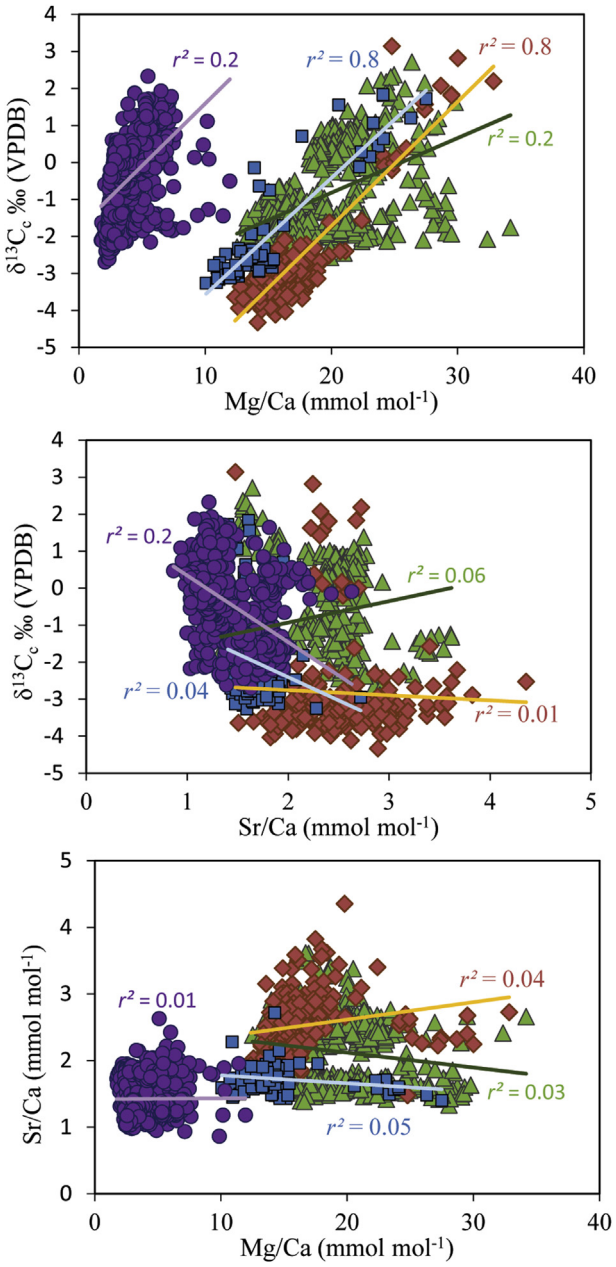

Fig. 4. Cross plots of Mg/Ca ratios, Sr/Ca ratios and $\delta^{13}C_c$ values from samples AB-DC-01 (blue), AB-DC-03 (red), AB-DC-09 (green) and AB-DC-12 (purple). Shown with a least squares linear regression and the coefficient of determination. Significant relationships were observed for samples AB-DC-01 and AB-DC-03 for Mg/Ca ratios and $\delta^{13}C_c$ values. (For interpretation of the references to colour in this figure legend, the reader is referred to the web version of this article.)

d). The Mg/Ca ratios varied between 10 and 34 mmol mol^{-1} with the exception of AB-DC-12, which ranged from 1.8 to 12 mmol mol^{-1} (Fig. 3 c). The Sr/Ca ratios ranged between 0.87 and 4.3 mmol mol^{-1} (Fig. 3 d). For sample AB-DC-09, increased Mg/Ca ratios were observed from 25.5 to 20 kyr BP, and from 31.7 to 30.7 kyr BP. There was no evidence in any of the stalagmites for a significant correlation between Sr/Ca and Mg/Ca ratios (Fig. 4). We observed a positive correlation between Mg/Ca ratios and $\delta^{13}C_c$ values ($r^2 = 0.8$, $p < 0.01$) from AB-DC-01 and AB-DC-03, but no significant correlation was found in AB-DC-09 or AB-DC-12 (Fig. 4). During the period of slow growth in stalagmite AB-DC-12, from 46.5 to 58.0 kyr BP, there does appear to be a slight anti-correlation between Mg/Ca ratios and $\delta^{13}C_c$ values, however this was not significant. In addition, no statistically significant correlation was observed between Sr/Ca ratios and $\delta^{13}C_c$ values (Fig. 4).

6. Discussion

6.1. What controls variations in oxygen and carbon isotopes?

The increased $\delta^{13}C_c$ and $\delta^{18}O_c$ values between ~62.5 and 60 ± 0.3, 48.5 to 46.5 ± 0.2, 40 to 38.5 ± 0.2, 31.7 to 30.5 ± 1, 25.5 to 23.6 ± 0.8 and 16.9 to 15 ± 0.5 kyr BP were associated with Heinrich stadials 1–6 (Fig. 5). The more negative $\delta^{13}C_c$ and $\delta^{18}O_c$ values were associated with D/O interstadials 3, 4, 8 to 12, and 16 to 18 and are on the order of ~0.5‰ (D/O stadial 4, 8, 9, 11, and 17) to ~1‰ (D/O stadial 3, 10, 12, 16, and 18) lower than preceding $\delta^{18}O_c$ and $\delta^{13}C_c$ values (Fig. 5). These changes in isotopic values are not as significant as those associated with Heinrich stadials.

The interpretation that changes in the $\delta^{13}C_c$ and $\delta^{18}O_c$ values were driven by climatic events is geochemically supported by the fact that multiple speleothems from the same cave record similar isotopic change during overlapping time intervals and the timing of the isotopic variations agree within the errors on the age models. Between 63.8 and 36.1 kyr BP there is only one record and therefore this period was not replicated. However given the similarities to other stalagmites, we propose the geochemical changes observed in AB-DC-12 are driven by climate.

Previous work using fluid inclusion isotopes indicated that the $\delta^{18}O_c$ values of the carbonate in AB-DC-09 stalagmite were primarily driven by temperature, rather than a change in the $\delta^{18}O$ of the source water, with an average temperature decline of ~4 °C across Heinrich stadials 1–3 (Arienzo et al., 2015). While no additional analyses were carried out as a result of the large amount of material needed for the fluid inclusion analysis, previous analyses demonstrate the $\delta^{18}O_w$ values across Heinrich stadials 1–3 did not significantly vary (Arienzo et al., 2015), and the records presented here exhibit similar $\delta^{18}O_c$ increases across Heinrich stadials (Fig. 5) supporting a similar temperature decline for all six Heinrich stadials. Conversely, the D/O interstadials are characterized by lower $\delta^{18}O_c$ values which therefore may be driven by a temperature increase or by changes in the $\delta^{18}O_w$ value of the drip water. When AB-DC-12 ceased forming, the $\delta^{18}O_c$ value was on average ~ −3.7‰ VPDB and the younger samples showed more positive $\delta^{18}O_c$ values (Fig. 3 a). This may be a result of differences in the drip water $\delta^{18}O_w$ values, water flow paths, or temperature variations within the cave. The interpretation of the carbon isotope record is inherently complex and therefore will be compared to the minor element results.

6.2. Minor elements: records of precipitation amount

Changes in Mg/Ca ratios of stalagmites are thought to arise from variations in Mg concentration of the bedrock, water/rock interactions, PCP, and temperature (Fairchild and Treble, 2009). In contrast to the shallower samples, AB-DC-01 and AB-DC-03 collected from 33.5 and 34.4 m below sea level, showed a high degree of correlation between Mg/Ca ratios and $\delta^{13}C_c$ values ($r^2 = 0.8$, $p < 0.01$, Fig. 4). Previous studies showed that dolomite was present on Abaco Island ~24 m below the surface (Kaldi and Gidman, 1982) and the two stalagmites (AB-DC-01 and AB-DC-03) with a high correlation between Mg/Ca and $\delta^{13}C_c$ values were located within this depth interval. Other studies on speleothems forming within dolomitic bedrock have demonstrated elevated Mg/Ca ratios and periods of lowered flow rates further elevated Mg/Ca ratios (Fairchild et al., 2000). The periods of higher Mg/Ca ratios and $\delta^{13}C_c$ values for stalagmites AB-DC-01 and AB-DC-03 were also associated with periods of decreased growth rates as indicated by

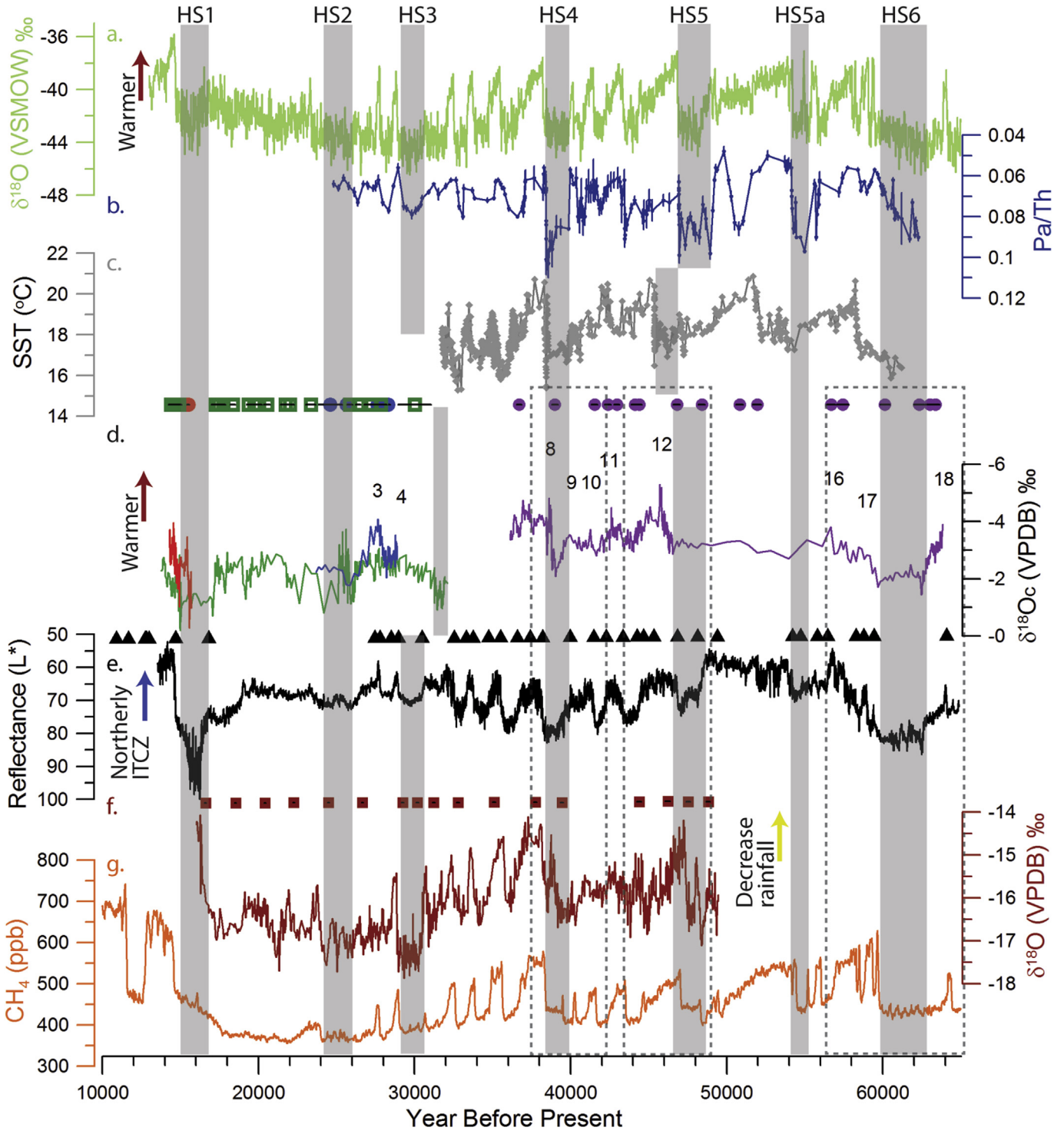

Fig. 5. Compilation of Atlantic paleo-records. NGRIP ice core $\delta^{18}O$ values (a) from Wolff et al. (2010) in green. Excess $^{231}Pa/^{230}Th$ (Pa/Th) in blue (b) from Bermuda Rise sediment core, axis reversed (Henry et al., 2016). Excess $^{231}Pa/^{230}Th$ is a proxy of AMOC strength, with increased Pa/Th indicating a reduced AMOC (Henry et al., 2016). Alkenone derived SST record from the Bermuda Rise (c) from Sachs and Lehman (1999), plotted in gray. Oxygen isotopes (d) from four Bahamas stalagmites (same as Fig. 3 a) plotted with the axis reversed. Stalagmite AB-DC-01 in blue, AB-DC-03 in red, AB-DC-09 in green, and AB-DC-12 in purple. The circles correspond to the U-Th dates for each of the stalagmite samples. Cariaco Basin reflectance data (e) in black from Deplazes et al. (2013), plotted with a 50 point running average and published tie points shown in black triangles. (f) Pacupahuain cave $\delta^{18}O$ calcite record from South America in red (Kanner et al., 2012) with U-Th dates in red squares. (g) CH_4 record in orange from the WAIS ice core from Rhodes et al. (2015) in orange. Each record is plotted on its own timescale. The gray bars represent the timing of Heinrich stadials (HS) and the numbers represent interstadials. The dotted boxes indicate the regions shown in Fig. 6. (For interpretation of the references to colour in this figure legend, the reader is referred to the web version of this article.)

the U-Th age models (Fig. 2). From these results we propose that the elevated Mg/Ca ratios and $\delta^{13}C_c$ values were likely driven by enhanced aridity which resulted in a reduction in the flow rate and increased water/rock interactions.

The periods of elevated Mg/Ca ratios and $\delta^{13}C_c$ values for both stalagmites AB-DC-01 and AB-DC-03 are coincident with Heinrich

stadials 1 and 2 suggesting that Heinrich stadials 1 and 2 in the Bahamas were potentially characterized by increased aridity as well as decreased temperature. The Mg/Ca ratios and $\delta^{13}C_c$ values for AB-DC-09 and AB-DC-12, did not show statistically significant correlations (Fig. 4a), although AB-DC-09 and AB-DC-12 exhibit increased $\delta^{13}C_c$ values across Heinrich stadials 1–6. We therefore tentatively propose the increased $\delta^{13}C_c$ values across Heinrich stadials 1–6 were potentially driven by increased aridity resulting in increased water/rock interactions and a lower biogenic CO_2 component of the DIC (Genty et al., 2003) in the Bahamas stalagmites.

In the case of AB-DC-09, increased Mg/Ca ratios were observed from 25.5 to 20 kyr BP and 31.7 to 30.7 kyr BP. These variations in the Mg/Ca record may in part be related to changes in the flow path of the water during periods of decreased flow rates (Fairchild and Treble, 2009). The overall lower Mg/Ca ratios in speleothem AB-DC-12 might be related to the fact that this stalagmite was the shallowest stalagmite collected, and therefore experienced lower amounts of water/rock interactions.

In contrast to Mg, the concentration of Sr remains relatively invariant in most of the stalagmites across Heinrich and D/O events. However, both stalagmites AB-DC-09 and AB-DC-03 exhibited higher Sr/Ca ratios starting at approximately 14.6 kyr BP. This has been interpreted as a period of higher amount of rainfall based on fluid inclusion $\delta^{18}O_w$ and $\delta^{18}O_c$ values (Arienzo et al., 2015). This possibly suggests that during wetter periods, the flow paths for the drip water changed, resulting in a greater Sr bedrock signature (Tooth and Fairchild, 2003). Some studies have also demonstrated that the incorporation of Sr in stalagmites can be influenced by variations in the growth rates (Huang and Fairchild, 2001; Lorens, 1981).

When analyzing for PCP, typically most studies utilized the covariability of Mg/Ca and Sr/Ca ratios (Fairchild and Treble, 2009; Treble et al., 2015). From the Mg/Ca and Sr/Ca ratios for the stalagmites analyzed here (Fig. 4c), we found no evidence of a significant relationship between the two ratios. This is in contrast to observations from other caves, in which Mg/Ca and Sr/Ca ratios typically co-vary (Fairchild and Treble, 2009). Therefore, we propose PCP is not a major driver of the trace element variability of these stalagmites.

7. Interpretation of paleoclimate results: comparison with Atlantic proxies

7.1. Heinrich stadials

The higher $\delta^{13}C_c$ and $\delta^{18}O_c$ values across Heinrich stadials 1–6 from the Bahamas stalagmites are shown to be in good agreement with other paleoproxies (Fig. 5) (Arienzo et al., 2015; Deplazes et al., 2013; Kanner et al., 2012; Peterson et al., 2000; Wang et al., 2001). The geochemical records from stalagmites presented in this paper, and from other proxies from the subtropical/tropical western Atlantic indicate that cooling occurred associated with Heinrich stadials (Arienzo et al., 2015; Grauel et al., 2016; Hagen and Keigwin, 2002; Hodell et al., 2012; Keigwin and Jones, 1994). The alkenone-derived sea surface temperature (SST) record from Bermuda (Fig. 1) showed a 3 to 5 °C decline in SSTs during Heinrich stadials thought to be driven by a reduction in the AMOC (Fig. 5 c) (Sachs and Lehman, 1999) which is supported by paleoproxies sensitive to AMOC strength (Henry et al., 2016, Fig. 5b). The Bahamas records suggest that an average ~4 °C decline occurred in the Bahamas across Heinrich stadials (Arienzo et al., 2015) which may be driven by a reduction in AMOC or due to associated increases in dust aerosols or clouds, which are a potential positive feedback on tropical Atlantic temperature (Murphy et al., 2014; Yuan et al., 2016).

In the Bahamas, the decline in temperature was likely accompanied by a decrease in the amount of precipitation during Heinrich stadials. Hosing experiments in modelling studies have proposed minimal changes in precipitation for this region (Clement and Peterson, 2008; Murphy et al., 2014; Zhang and Delworth, 2005). Yet further south of the Bahamas, records of stable isotopes, gypsum hydration waters, and clumped isotopes from Guatemala show temperatures declined during Heinrich stadials by 5–10 °C relative to the Holocene and aridity increased (Escobar et al., 2012; Grauel et al., 2016; Hodell et al., 2012). The sediment core records from Cariaco Basin also support an increased aridity during Heinrich stadials (Fig. 5 e) (Deplazes et al., 2013; Peterson et al., 2000). The increased aridity associated with Heinrich stadials in the Bahamas was potentially driven by reduced AMOC in the North Atlantic, an expanded Bermuda High and a southerly shifted ITCZ (Deplazes et al., 2013; Grauel et al., 2016; Hodell et al., 2012).

When comparing between various records from the Atlantic, the differences between Heinrich stadials becomes evident. The Bahamas and Guatemala records both support Heinrich stadial 1 was the most extreme event (Escobar et al., 2012; Grauel et al., 2016; Hodell et al., 2012). The Bahamas records also showed significant geochemical variations associated with Heinrich stadials 2, 4 and 6. Heinrich stadials 1, 2, 4 and 5 were potentially sourced from the Hudson Straits (Hemming, 2004; Hodell et al., 2008) and were characterized by the greatest AMOC reductions (Fig. 5 b) (Henry et al., 2016). Conversely, Heinrich stadials 3, 5 and 5a were not well defined events in the geochemistry of the Bahamas records. This may in part be because of the reduced growth rate during Heinrich stadials 5 and 5a. However, the Cariaco Basin record also demonstrated a minimal response to Heinrich stadial 3 and 5a (Deplazes et al., 2013), both of which have a mixed North Atlantic provenance (Hodell et al., 2008; Rhodes et al., 2015). In addition, Heinrich stadial 3 does not exhibit a significant change in AMOC strength (Henry et al., 2016). Such differences between Heinrich stadials and the observed agreement between various paleoclimate proxies support the strength of the AMOC and the source of freshwater to the North Atlantic were important parameters for the global propagation of stadial events (Hemming, 2004; Rhodes et al., 2015; Henry et al., 2016).

7.2. Interstadials

The more negative $\delta^{13}C_c$ and $\delta^{18}O_c$ values from the Bahamas stalagmites associated with D/O interstadials 3, 4, 8 to 12, and 16 to 18, occur coincident with other records such as Greenland ice cores (Wolff et al., 2010), Cariaco Basin (Deplazes et al., 2013) and South American speleothems (Kanner et al., 2012) (Fig. 5). The more negative $\delta^{13}C_c$ and $\delta^{18}O_c$ values (Fig. 5 d) suggest warmer and/or wetter conditions for the Bahamas during interstadials and are in agreement with proxy data from the Cariaco Basin sediments. The Cariaco sediment records support a wetter climate across D/O interstadials thought to be driven by the northerly shift in the ITCZ during interstadials (Fig. 5 e) (Deplazes et al., 2013; Peterson et al., 2000), and warmer SSTs in the Northern Hemisphere, as supported by the Bermuda Rise record (Sachs and Lehman, 1999; Wolff et al., 2010) (Fig. 5 a and c).

The NGRIP and Bermuda Rise records demonstrated a characteristic saw-tooth pattern during D/O events, with rapidly increasing temperatures followed by a steady decline (Fig. 5 a and c). This pattern was particularly evident from the NGRIP dataset for D/O interstadials 8, 10, 11, and 12 (Fig. 5 a). Deplazes et al. (2013) noted that the Cariaco Basin record does not contain the saw-tooth pattern for D/O cycles observed at higher latitudes which was also not observed in this study (Figs. 5 and 6), rather the

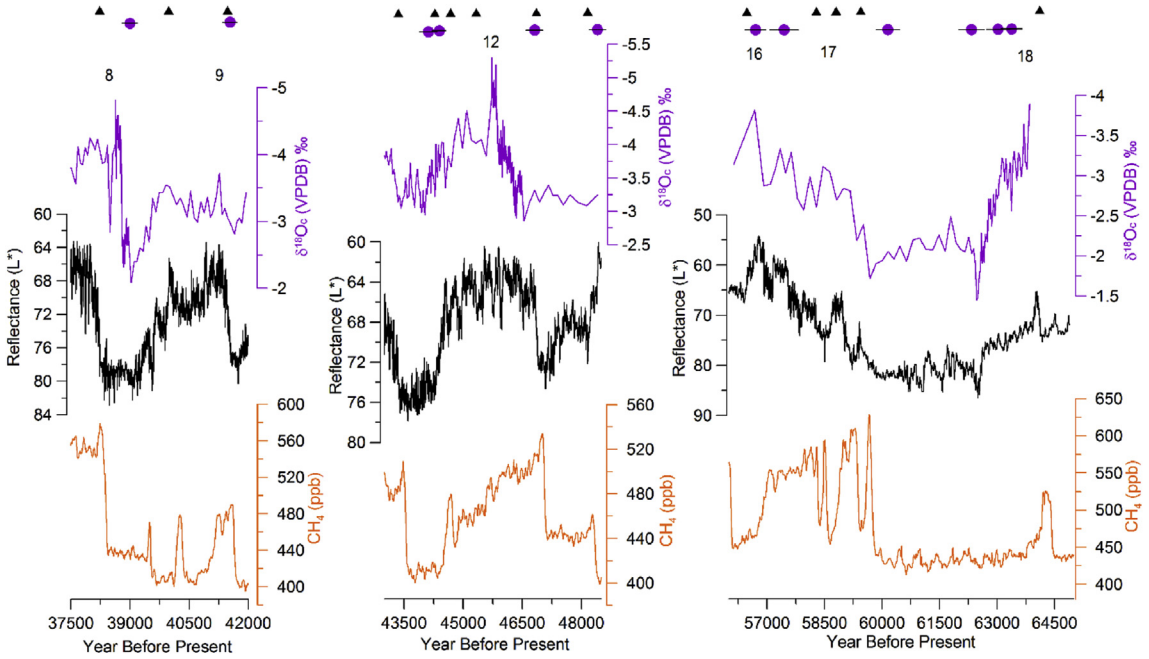

Fig. 6. Compilation of Atlantic paleo-records over Heinrich stadials 4 (left), 5 (middle) and 6 (right). Oxygen isotopes from AB-DC-12 in purple with the axis reversed. Cariaco Basin reflectance data in black from Deplazes et al. (2013), plotted with a 50 point running average. CH_4 record in orange from the WAIS ice core from Rhodes et al. (2015). Each record is plotted on its own timescale. U-Th ages for AB-DC-12 are shown as purple circles and the published tie points for the Cariaco Basin record are shown as black triangles at the top of the figure with published errors (Deplazes et al., 2013). (For interpretation of the references to colour in this figure legend, the reader is referred to the web version of this article.)

transitions to D/O interstadials appear to be more gradual than the higher latitude records. In the Bahamas, the minimal isotopic shift associated with D/O events may be driven by a reduced climate response in the Bahamas to D/O events possibly a result of the mechanism that propagates the D/O events globally (Deplazes et al., 2013; Li et al., 2010; Menviel et al., 2014).

7.3. Centennial scale

The Cariaco Basin record from Deplazes et al. (2013) and the Bahamas records show periods of agreement on the centennial scale during rapid climate change events. For example, both records demonstrate a similar increase in the beginning of Heinrich stadial 6 at ~62.3 kyr BP and similar variability within Heinrich stadial 6, D/O cycles 12 to 9, and at ~44 and 41 kyr BP (Figs. 5 and 6). Similar centennial scale variability was observed in the Pacupahuain oxygen isotope record (Kanner et al., 2012) as well as the methane (CH_4) record from the West Antarctic Ice Sheet (WAIS) Divide ice core (Rhodes et al., 2015), particularly associated with the onset of the stadial events (Fig. 6). The Bahamas stalagmite AB-DC-12 exhibited a reduced growth rate from 58 to 48 kyr BP which makes comparisons to this record difficult over this time period (Fig. 5). We also note that discrepancies do exist, for example a decrease in the Bahamas $\delta^{18}O_c$ record at ~38 kyr BP while the Cariaco Basin shows no changes. However, such centennial scale agreements may potentially be linked to variations in the Northern Hemisphere high latitude climate, iceberg discharge or AMOC variations which is supported by the observed agreement across several paleoproxies. To more fully understand the mechanistic linkages resulting in such coherence, additional high resolution, absolutely dated paleoclimate records from the low latitudes are needed to further confirm the cohesiveness of this regional signal.

8. Conclusions

Through the application of various geochemical proxies on multiple speleothems forming over the last 64,000 years, millennial climate variations have been resolved, including Heinrich stadials 1 to 6. From the analysis of the carbon and oxygen isotopes, higher values were associated with Heinrich stadials 1–6. The $\delta^{18}O_c$ record was proposed to be a result of lower temperatures across the stadial events (Arienzo et al., 2015). The minor element data showed higher water/rock interactions during Heinrich stadials based on co-varying Mg/Ca ratios and $\delta^{13}C_c$ values from two stalagmites. Covariation was proposed to be a result of reduced flow rates in the epikarst driven by a more arid climate associated with Heinrich stadials. All stalagmites show increased $\delta^{13}C_c$ values associated with Heinrich stadials attributed to enhanced aridity.

Through comparisons to paleoclimate record from the Atlantic, we showed the observed climatic changes are driven by largescale shifts in the climate system driven by the AMOC. The robust relationship between tropical paleoclimate records from the Bahamas, Cariaco Basin and Guatemala supports the influence of climate variation in the high latitude Northern Hemisphere on the tropics on the millennial to centennial scale. During Heinrich stadials, reduced SSTs, a southerly shifted ITCZ, and expanded Bermuda High resulted in lower temperatures and enhanced aridity. The variations in the geochemical response associated with each Heinrich stadial supports the AMOC reduction and the source of freshwater to the North Atlantic are both important parameters for the global propagation of the stadial events. During D/O interstadials, lower $\delta^{13}C_c$ and $\delta^{18}O_c$ values were thought to be a result of warmer and/or wetter climate; however the isotopic shifts were not as significant as the isotopic excursions associated with Heinrich stadials, possibly indicating D/O events were not significant climate events in the Bahamas or the events were not well recorded in speleothem geochemistry.

Acknowledgements

This research was supported with funds from NSF grant AGS-1103489 (PKS, AC, KB, and AP), AC received additional support from

NSF P2C2 award # 1304540, a Cave Research Foundation Graduate Research Grant to MMA and The National Geographic Society Grant #EC0428-09 to KB and BK. The authors would like to thank Sevag Mehterian and the members of the Stable Isotope Laboratory at the University of Miami for their help with data collection. The authors would also like to thank the two anonymous reviewers for their constructive feedback. Geochemical data are available at the NOAA Paleoclimate website.

Appendix A. Supplementary data

Supplementary data related to this article can be found at http://dx.doi.org/10.1016/j.quascirev.2017.02.004.

References

Arienzo, M.M., Swart, P.K., Pourmand, A., Broad, K., Clement, A.C., Murphy, L.N., Vonhof, H.B., Kakuk, B., 2015. Bahamas speleothem reveals climate variability associated with Heinrich events. Earth Planet. Sci. Lett. 430, 377–386.

Baldini, L.M., Walker, S.E., Railsback, L.B., Baldini, J.U.L., Crowe, D.E., 2007. Isotopic ecology of the modern land snail Cerion, San Salvador, Bahamas: preliminary advances toward establishing a low-latitude island paleoenvironmental proxy. Palaios 22, 174–187.

Beck, J.W., Richards, D.A., Edwards, R.L., Silverman, B.W., Smart, P.L., Donahue, D.J., Hererra-Osterheld, S., Burr, G.S., Calsoyas, L., Jull, A.J., Biddulph, D., 2001. Extremely large variations of atmospheric 14C concentration during the last glacial period. Science 292, 2453–2458.

Bond, G., Showers, W., Cheseby, M., Lotti, R., Almasi, P., deMenocal, P., Priore, P., Cullen, H., Hajdas, I., Bonani, G., 1997. A pervasive millennial-scale cycle in North Atlantic Holocene and glacial climates. Science 278, 1257–1266.

Breitenbach, S., Rehfeld, K., Goswami, B., Baldini, J., Ridley, H., Kennett, D., Prufer, K., Aquino, V., Asmerom, Y., Polyak, V., Cheng, H., Kurths, J., Marwan, N., 2012. COnstructing proxy records from age models (COPRA). Clim. Past 8, 1765–1779.

Broecker, W.S., Peteet, D.M., Rind, D., 1985. Does the ocean-atmosphere system have more than one stable mode of operation. Nature 315, 21–26.

Buizert, C., Schmittner, A., 2015. Southern Ocean control of glacial AMOC stability and Dansgaard-Oeschger interstadial duration. Paleoceanography 30.

Clement, A.C., Cane, M.A., 1999. A role for the tropical pacific coupled ocean-atmosphere system on Milankovitch and millennial timescales. In: Clark, P.U., Webb, R.S., Keigwin, L.D. (Eds.), Mechanisms of Global Climate Change at Millennial Time Scales. AGU, Washington, D.C, pp. 363–371.

Clement, A.C., Peterson, L.C., 2008. Mechanisms of abrupt climate change of the last glacial period. Rev. Geophys. 46.

Cross, M., McGee, D., Broecker, W., Quade, J., Shakun, J., Cheng, H., Lu, Y., Edwards, R., 2015. Great Basin Hydrology, Paleoclimate, and Connections with the North Atlantic: a Speleothem Stable Isotope and Trace Element Record from Lehman Caves, NV.

Cruz, F., Burns, S., Jercinovic, M., Karmann, I., Sharp, W., Vuille, M., 2007. Evidence of rainfall variations in Southern Brazil from trace element ratios (Mg/Ca and Sr/Ca) in a Late Pleistocene stalagmite. Geochim. Cosmochim. Acta 71, 2250–2263.

Dansgaard, W., Johnsen, S.J., Clausen, H.B., Dahl-Jensen, D., Gundestrup, N., Hammer, C.U., Oeschger, H., 1984. North Atlantic Climatic Oscillations Revealed by Deep Greenland Ice Cores, Climate Processes and Climate Sensitivity. AGU, p. 10.

Deplazes, G., Luckge, A., Peterson, L.C., Timmermann, A., Hamann, Y., Hughen, K.A., Rohl, U., Laj, C., Cane, M.A., Sigman, D.M., Haug, G.H., 2013. Links between tropical rainfall and North Atlantic climate during the last glacial period. Nat. Geosci. 6, 213–217.

Dorale, J.A., Liu, Z.H., 2009. Limitations of Hendy Test criteria in judging the paleoclimatic suitability of speleothems and the need for replication. J. Cave Karst Stud. 71, 73–80.

Escobar, J., Hodell, D.A., Brenner, M., Curtis, J.H., Gilli, A., Mueller, A.D., Anselmetti, F.S., Ariztegui, D., Grzesik, D.A., Pérez, L., Schwalb, A., Guilderson, T.P., 2012. A ~43-ka record of paleoenvironmental change in the Central American lowlands inferred from stable isotopes of lacustrine ostracods. Quat. Sci. Rev. 37, 92–104.

Fairchild, I.J., Baker, A., 2012. Speleothem Science: from Processes to Past Environments. Wiley-Blackwell.

Fairchild, I.J., Borsato, A., Tooth, A.F., Frisia, S., Hawkesworth, C.J., Huang, Y.M., McDermott, F., Spiro, B., 2000. Controls on trace element (Sr-Mg) compositions of carbonate cave waters: implications for speleothem climatic records. Chem. Geol. 166, 255–269.

Fairchild, I.J., Smith, C.L., Baker, A., Fuller, L., Spötl, C., Mattey, D., McDermott, F., E.I.M.F, 2006. Modification and preservation of environmental signals in speleothems. Earth Sci. Rev. 75, 105–153.

Fairchild, I.J., Treble, P.C., 2009. Trace elements in speleothems as recorders of environmental change. Quat. Sci. Rev. 28, 449–468.

Fletcher, W.J., Sánchez Goñi, M.F., Allen, J.R.M., Cheddadi, R., Combourieu-Nebout, N., Huntley, B., Lawson, I., Londeix, L., Magri, D., Margari, V., Müller, U.C., Naughton, F., Novenko, E., Roucoux, K., Tzedakis, P.C., 2010. Millennial-scale variability during the last glacial in vegetation records from Europe. Quat. Sci. Rev. 29, 2839–2864.

Genty, D., Blamart, D., Ouahdi, R., Gilmour, M., Baker, A., Jouzel, J., Van-Exter, S., 2003. Precise dating of Dansgaard-Oeschger climate oscillations in western Europe from stalagmite data. Nature 421, 833–837.

Grauel, A.L., Hodell, D.A., Bernasconi, S.M., 2016. Quantitative estimates of tropical temperature change in lowland Central America during the last 42 ka. Earth Planet Sci. Lett. 438, 37–46.

Grimm, E.C., Watts, W.A., Jacobson Jr., G.L., Hansen, B.C.S., Almquist, H.R., Dieffenbacher-Krall, A.C., 2006. Evidence for warm wet heinrich events in Florida. Quat. Sci. Rev. 25, 2197–2211.

Hagen, S., Keigwin, L.D., 2002. Sea-surface temperature variability and deep water reorganisation in the subtropical North Atlantic during Isotope Stage 2-4. Mar. Geol. 189, 145–162.

Hemming, S.R., 2004. Heinrich events: massive late Pleistocene detritus layers of the North Atlantic and their global climate imprint. Rev. Geophys. 42.

Hendy, C.H., 1971. Isotopic geochemistry of speleothems .1. Calculation of effects of different modes of formation on isotopic composition of speleothems and their applicability as palaeoclimatic indicators. Geochim. Cosmochim. Acta 35, 801-&.

Henry, L., McManus, J.F., Curry, W.B., Roberts, N.L., Piotrowski, A.M., Keigwin, L.D., 2016. North Atlantic ocean circulation and abrupt climate change during the last glaciation. Science 35 (6298), 470–474.

Hodell, D.A., Turchyn, A.V., Wiseman, C.J., Escobar, J., Curtis, J.H., Brenner, M., Gilli, A., Mueller, A.D., Anselmetti, F., Ariztegui, D., Brown, E.T., 2012. Late Glacial temperature and precipitation changes in the lowland Neotropics by tandem measurement of delta O-18 in biogenic carbonate and gypsum hydration water. Geochim. Cosmochim. Acta 77, 352–368.

Hodell, D.A., Channell, J.E.T., Curtis, J.H., Romero, O.E., Rohl, U., 2008. Onset of "Hudson strait" Heinrich events in the eastern north Atlantic at the end of the middle pleistocene transition (~640 ka)? Paleoceanography 23.

Hoffmann, D.L., Beck, J.W., Richards, D.A., Smart, P.L., Singarayer, J.S., Ketchmark, T., Hawkesworth, C.J., 2010. Towards radiocarbon calibration beyond 28ka using speleothems from the Bahamas. Earth Planet. Sci. Lett. 289, 1–10.

Huang, Y.M., Fairchild, I.J., 2001. Partitioning of Sr2+ and Mg2+ into calcite under karst-analogue experimental conditions. Geochim. Cosmochim. Acta 65, 47–62.

Jiménez-Moreno, G., Anderson, R.S., Desprat, S., Grigg, L.D., Grimm, E.C., Heusser, L.E., Jacobs, B.F., López-Martínez, C., Whitlock, C.L., Willard, D.A., 2010. Millennial-scale variability during the last glacial in vegetation records from North America. Quat. Sci. Rev. 29, 2865–2881.

Jouzel, J., Masson-Delmotte, V., Cattani, O., Dreyfus, G., Falourd, S., Hoffmann, G., Minster, B., Nouet, J., Barnola, J.M., Chappellaz, J., Fischer, H., Gallet, J.C., Johnsen, S., Leuenberger, M., Loulergue, L., Luethi, D., Oerter, H., Parrenin, F., Raisbeck, G., Raynaud, D., Schilt, A., Schwander, J., Selmo, E., Souchez, R., Spahni, R., Stauffer, B., Steffensen, J.P., Stenni, B., Stocker, T.F., Tison, J.L., Werner, M., Wolff, E.W., 2007. Orbital and millennial Antarctic climate variability over the past 800,000 years. Science 317, 793–796.

Kaldi, J., Gidman, J., 1982. Early diagenetic dolomite cements - examples from the permian lower magnesian limestone of England and the pleistocene carbonates of the Bahamas. J. Sediment. Petrol 52, 1073–1085.

Kanner, L.C., Burns, S.J., Cheng, H., Edwards, R.L., 2012. High-latitude forcing of the south American summer monsoon during the last glacial. Science 335, 570–573.

Keigwin, L.D., Jones, G.A., 1994. Western North-Atlantic evidence for millennial-scale changes in ocean circulation and climate. J. Geophys. Res. Oceans 99, 12397–12410.

Lambert, W.J., Aharon, P., 2011. Controls on dissolved inorganic carbon and delta C-13 in cave waters from DeSoto Caverns: implications for speleothem delta C-13 assessments. Geochim. Cosmochim. Acta 75, 753–768.

Li, C., Battisti, D.S., Bitz, C.M., 2010. Can North Atlantic sea ice anomalies account for Dansgaard-Oeschger climate signals. J. Clim. 23, 5457–5475.

Lorens, R.B., 1981. Sr, Cd, Mn and Co distribution coefficients in calcite as a function of calcite precipitation rate. Geochim. Cosmochim. Acta 45, 553–561.

Lozano-Garcia, S., Ortega, B., Roy, P., Beramendi-Orosco, L., Caballero, M., 2015. Climatic variability in the northern sector of the American tropics since the latest MIS 3. Quat. Res.

McManus, J.F., Francois, R., Gherardi, J.M., Keigwin, L.D., Brown-Leger, S., 2004. Collapse and rapid resumption of Atlantic meridional circulation linked to deglacial climate changes. Nature 428, 834–837.

Menviel, L., Timmermann, A., Friedrich, T., England, M.H., 2014. Hindcasting the continuum of Dansgaard-Oeschger variability: mechanisms, patters and timing. Clim. Past 63–77.

Mühlinghaus, C., Scholz, D., Mangini, A., 2009. Modelling fractionation of stable isotopes in stalagmites. Geochim. Cosmochim. Acta 73, 7275–7289.

Murphy, L.N., Clement, A.C., Albani, S., Mahowald, N.M., Swart, P.K., Arienzo, M.M., 2014. Simulated changes in atmospheric dust in response to a Heinrich stadial. Paleoceanography 29, 30–43.

Petersen, S.V., Schrag, D., Clark, P.U., 2013. A new mechanism for Dansgaard-Oeschger cycels. Paleoceanography 28, 24–30.

Peterson, L.C., Haug, G.H., Hughen, K.A., Rohl, U., 2000. Rapid changes in the hydrologic cycle of the tropical Atlantic during the last glacial. Science 290, 1947–1951.

Pourmand, A., Tissot, F.L.H., Arienzo, M.M., Sharifi, A., 2014. Introducing a comprehensive data reduction and uncertainty propagation algorithm for U-Th geochronometry with extraction chromatography and isotope dilution MC-ICP-MS. Geostand. Geoanal. Res. 38, 129–148.

Rhodes, R.H., Brook, E.J., Chiang, J.C.H., Blunier, T., Maselli, O.J., McConnell, J.R., Romanini, D., Severinghaus, J.P., 2015. Enhanced tropical methane production in response to iceberg discharge in the North Atlantic. Science 348, 1016–1019.
Sachs, J.P., Lehman, S.J., 1999. Subtropical North Atlantic temperatures 60,000 to 30,000 years ago. Science 286, 756–759.
Siddall, M., Rohling, E.J., Blunier, T., Spahni, R., 2010. Patterns of millennial variability over the last 500 ka. Clim. Past 6, 295–303.
Timmermann, A., Gildor, H., Schulz, M., Tziperman, E., 2003. Coherent resonant millennial-scale climate oscillations triggered by massive meltwater pulses. J. Clim. 16, 2569–2585.
Tooth, A.F., Fairchild, I.J., 2003. Soil and karst aquifer hydrological controls on the geochemical evolution of speleothem-forming drip waters, Crag cave, Southwest Ireland. J. Hydrol. 273, 51–68.
Treble, P., Fairchild, I.J., Griffiths, A., Baker, A., Meredith, K.T., Wood, A., McGuire, E., 2015. Impacts of cave air ventilation and in-cave prior calcite precipitation on Golgotha cave dripwater chemistry, Southwest Autralia. Quat. Sci. Rev. 127, 61–72.
Tremaine, D.M., Froelich, P.N., 2013. Speleothem trace element signatures: a hydrologic geochemical study of modern cave dripwaters and farmed calcite. Geochim. Cosmochim. Acta 121, 522–545.
Tremaine, D.M., Froelich, P.N., Wang, Y., 2011. Speleothem calcite farmed in situ: modern calibration of δ18O and δ13C paleoclimate proxies in a continuously-monitored natural cave system. Geochim. Cosmochim. Acta 75, 4929–4950.
Walker, L.N., Mylroie, J.E., Walker, A.D., Mylroie, J.R., 2008. The caves of Abaco island, Bahamas: keys to geologic timelines. J. Cave Karst Stud. 70, 108–119.
Wang, Y.J., Cheng, H., Edwards, R.L., An, Z.S., Wu, J.Y., Shen, C.C., Dorale, J.A., 2001. A high-resolution absolute-dated late Pleistocene monsoon record from Hulu Cave, China. Science 294, 2345–2348.
Wolff, E.W., Chappellaz, J., Blunier, T., Rasmussen, S.O., Svensson, A., 2010. Millennial-scale variability during the last glacial: the ice core record. Quat. Sci. Rev. 29, 2828–2838.
Wong, C.I., Banner, J.L., Musgrove, M., 2011. Seasonal dripwater Mg/Ca and Sr/Ca variations driven by cave ventilation: implications for and modeling of speleothem paleoclimate records. Geochim. Cosmochim. Acta 75, 3514–3529.
Yuan, T., Oreopoulos, L., Zelinka, M., Yu, H., Norris, J.R., Chin, M., Platnick, S., Meyer, K., 2016. Positive low cloud and dust feedbacks amplify tropical North Atlantic multidecadal oscillation. Geophys. Res. Lett. 43, 1349–1356.
Zhang, R., Delworth, T.L., 2005. Simulated tropical response to a substantial weakening of the Atlantic thermohaline circulation. J. Clim. 18, 1853–1860.